# LMECA2840 - Project in mechanical design
# Technical Report III :


| | |
|---|---|
| Brevi Matteo | 7708-16-00 |
| Creelle Robbe | 3693-17-00 |
| Diriken Axel | 3382-17-00 |
| Ibrahim Muhammad | 1444-20-00 |
| Marchal Youri | 6170-17-00 |
| Peres Hugo | 4454-16-00 |
| Philipin Aurélien | 4622-17-00 |


March 19, 2021 - Group A5

# Contents

# 1 Introduction

Our task is to design a rolling overhead crane in the hangar where the assembly of the SEAGLE will take place. The SEAGLE is a fire fighting plane that will be able to refill its water tank very quickly by flying/floating at the water surface thanks to its foils. The overhead crane should be able to lift up to 15 tons and should be flexible to smaller piece. Furthemore, it should be precise enough in order to position the parts correctly to assemble the parts together. The dimensions of the hangar are pretty large and this is one of the few things that is making the project so challenging as well.
In the preliminary layout, we only used one cable at the center of the trolley to lift the parts, but we faced the problem that large pieces would start to swing as soon as the crane starts to move with them due to inertia. This is why we decided to multiply the number of lifting cables and to the push them aside to reduce that swinging effect.

# 2 Current layout

There are two main differences between the current and the previous layout, the first one is the lifting up system which is composed by an unique cable but which is connecting pulleys on the top platform with other pulleys on the bottom platform as shown on the figure 2 and 3. The two main purposes why we kept only one continuous cable instead of 4 independent ones are to use only one motor for the lifting up, which allow us to not have synchronization problems between different motors. The second purpose is to divide the force required to lift up the bottom platform and the piece attach to it. Indeed pulleys allow us to use less force for lifting the same mass. The previous layout was composed only with a hook and four cables with a fixed length as you can see on the figure 1.

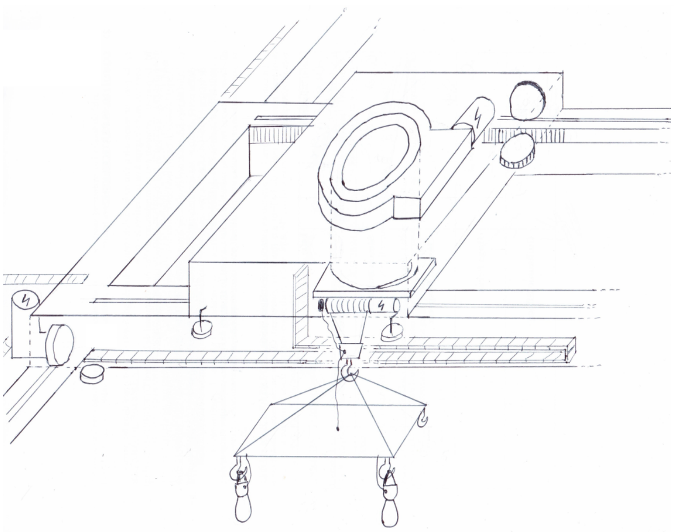

Figure 1: Previous layout

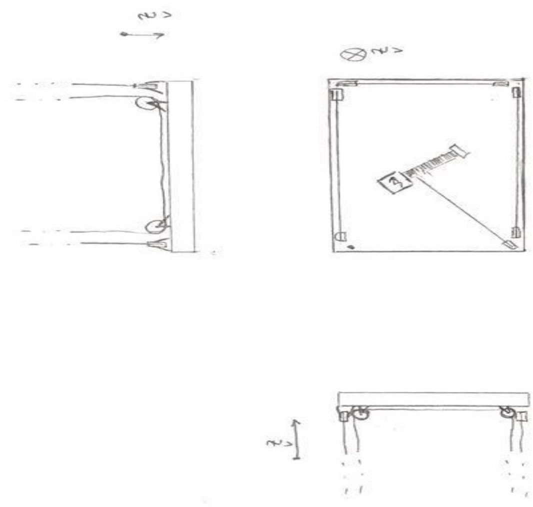

Figure 2: Current lifting up system : Bottom view

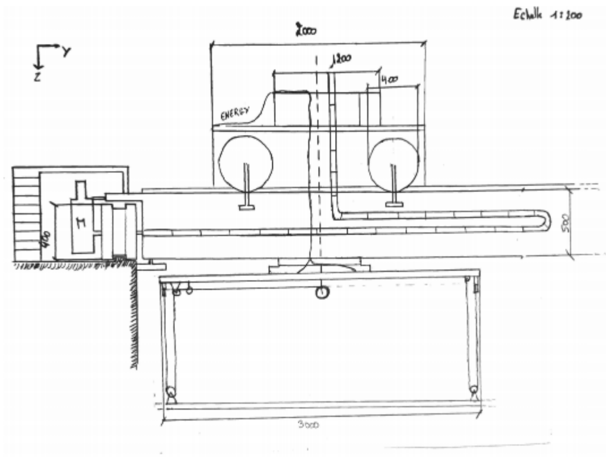


Figure 3: Current layout

The second main difference is the shape of the trolley and the platforms which now have an H-shape as shown in the following sections. The idea was to minimize the mass of the two devices which had a rectangular shape in the previous layout as you can see on the figure 1.

# 3 Dimensioning

## 3.1 Efforts analysis

The efforts on the rolling bridge will propagate along the structure as you can see on figure 4

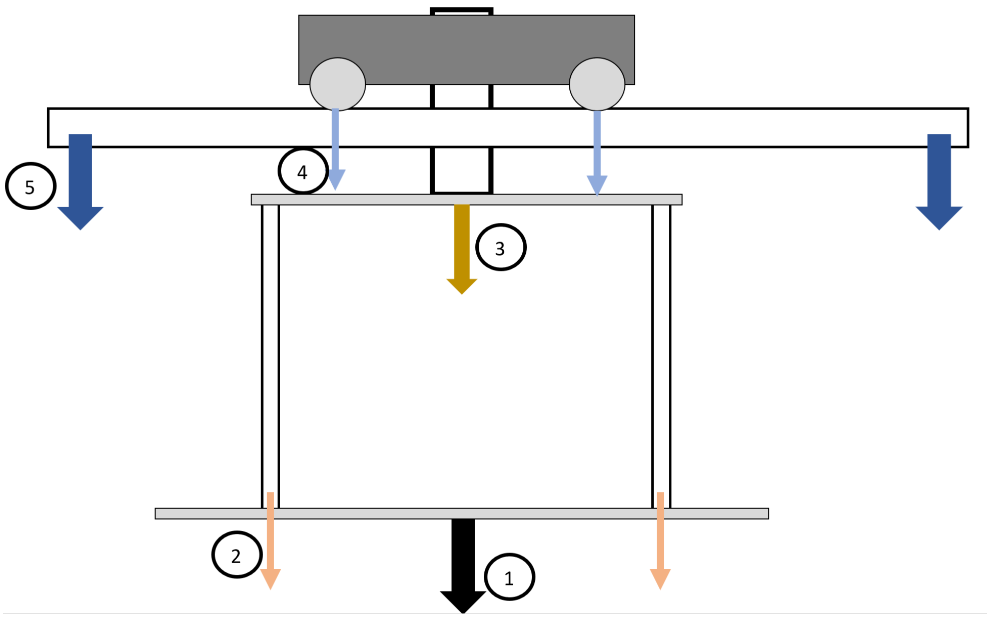


Figure 4: effort inside the structure

1. The load of the piece which is being lifted (15 tons maximum) acting on the horizontal platform.
2. The tension applied on the cables.
3. The vertical load on the vertical column.
4. The loads that are being transmitted to the transverse beams through the wheels of the trolley.
5. The efforts on the rollers that are going to be needed to support the beams with the trolley

Of course, the loads add up, for example, load *3* corresponds to the sum of the load of the piece, the load of the platform and the load of the cables.
In the following sections, we will study the dimensions of each part.

## 3.2 Platform

**Assumptions**

- $\gamma = 2$ : We chose a value for the security factor of 2. This value has been chosen after reading *section 6.12.2* in the Juvinall [10] textbook. We assumed that we have an "*average material operating in an ordinary environment and subjected to loads and stresses that can be determined*"
- We assumed that the maximum weight of 15 tons will be applied at one single point in the middle of the platform. In reality, this will never happen as we ask the costumer to have a minimal number of 3 attaching points for such heavy pieces. The weight will also not necessarly be applied in the middle of the platform, but as this is the most critical location, we decided to apply it there for the dimensioning.
- As a material we chose AISI1022 steel with:
  - $\rho = 7860$ [kg/m$^3$]
  - $\sigma_y = 360$ [MPa]

  To get these values, we looked what kind of steel we should select in the *Juvinal* textbook[10] and as the platform was a structural part, we decided to pick a low carbon steel. From there we found AISI1022 to be a good solution for our application. We obtained its mechanical properties from *Matweb* website. [2]

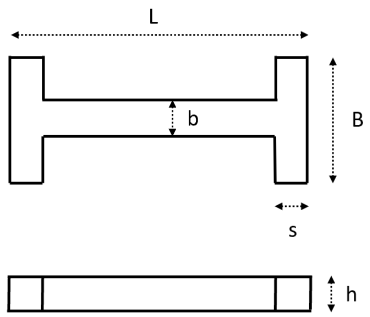


Figure 5: Schematic of the platform + notations

- For the calculation of the needed height we decided to simplify te shape to a reclangle with dimensions $h, b, L$ (see figure 5). So the inertia of the section will be $I = \frac{bh^3}{12}$. The H shape allows to save significant weight though and we still can have attaching points at the 4 corners of the platform.
- Shear stress and axial loading is considered very small compared to the stress induced by the bending moment

**Calculations**

As you can see on figure 6, the maximum bending moment undergone by the platform is $M_{max} = \frac{FL}{4}$. The stress in the section due to bending is also evolving through the height $h$ of the section. It is at its extremum value at the top and bottom edge and is equal to zero at the center, therefore the maximum stress undergone by the platform is:

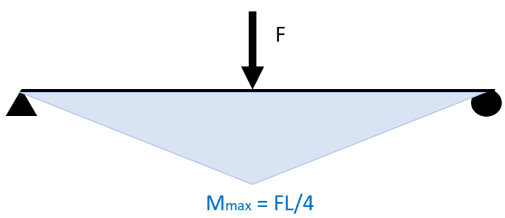


Figure 6: Internal stress

$$\sigma_{max} = \frac{M_{max} \cdot h/2}{I} = \frac{\frac{FL}{4} \cdot h/2}{\frac{bh^3}{12}} = \frac{3FL}{2bh^2}$$

In order to stay in the elastic regime of the platform, we want $\sigma_y > \gamma\sigma_{max}$. And from there we can calculate the height of the platform:

$$\sigma_y > \gamma\sigma_{max}$$
$$\sigma_y > \gamma \cdot \frac{3FL}{2bh^2}$$
$$h > \sqrt{\frac{3\gamma FL}{2b\sigma_y}}$$

And we can deduce the weight knowing the shape (see figure 5):

$$W_{Platform} = \rho \cdot (bhL + 2(B-b)hs) \tag{1}$$

If we fix the values of $L = 3m$, $b = 0.3m$, $s = 0.2$ and $B = 1.5m$, we obtain for h and for the weight:

$$h = 0.13 \quad m$$
$$W_{Platform} = 1410 \quad kg$$

## 3.3 Cables

**Assumptions**

- The cables only undergo traction
- The weight is uniformly distributed into 8 different supporting parts of the cable thanks to a pulley system
- $\gamma = 5$. As stated in the following website, we decided to take a security factor of 5 for the lifting cables.[1]
- The characteristics for the lifting cables are:
  - $\sigma_y = 1700$ [MPa]
  - linear density $w_l$ depends on the result of the diameter. [3]

**Calculations**
The maximum stress undergone in the cable is tension expressed as $\sigma_{max} = \frac{F}{A}$, where F is the pulling force and A the surface of the section. (Do not forget that the pulling force is actually only $\frac{1}{8}$ of the weight that is below the cable). Therefore:

$$D_{min} = \sqrt{\gamma \frac{4F}{\pi \sigma_y}}$$
$$\text{where } F = \frac{W_{piece} + W_{Platform}}{8} \cdot g$$

As it is a cable, we will select a slightly different section (stranded wire), the procedure is actually a bit different and we will select a diameter based on the maximum tension force allowed on a cable that we find on the *rgm cranes* website: [3]. From there we obtain that we should take a cable with diameter $D = 19\,mm$ as our tensile force is $F = 161\,kN$, which leads to a linear weight of $\dot{w} = 1.41\,\frac{kg}{m}$, so $W_{cable} = \dot{w} \cdot 150 = 212\,kg$.

## 3.4 Vertical cylinder

The slewing ring permits to rotate the platform in the z-direction. It consists of a hollow ring which rotates via a motor acting on a screw worm (vis sans fin). The slewing ring is attached to a hollow cylinder which transmits the efforts to the cables.
A slewing ring can be chosen by various manufacturers. Before choosing, it is needed to define the critical dimensions of this cylinder.
First of all, there is some tension due the weight of the piece, the platform and the slewing ring itself. The cables are neglected due to their low weight with respect to the other components of the trolley.
Secondly, there is some torsion due to the inertia of all the parts during starting or stopping of the rotation.
Thirdly, the cylinder is put on the trolley which moves in the y or x direction. If it stops abruptly, there is a risk the cylinder fails due to bending.

**Assumptions**

- The cylinder has an outer radius of D and inner of d. The ratio $D/d$ is $\phi$.
- For the calculations, the height of the cylinder is $h = 2m$.
- As a material we chose AISI1022 steel with:
  - $\rho = 7860$ [kg/m$^3$]
  - $\sigma_y = 360$ [MPa]

- Axial acceleration (rotation acceleration): $\dot{\alpha} = 8.72 \cdot 10^{-3}$ $[rad/s^2]$
This acceleration has been chosen as the maximal rotational speed along z of the slewing ring is 1 $[deg/s]$ ($8.72 \cdot 10^{-3}$ $[rad/s^2]$) and we ant the device to be able to accelerate to that speed in $1s$.

- $W_{piece} = 15000$ $[kg]$ : maximum mass of the piece

- $W_{plat} = 1410$ $[kg]$ and $W_{cables} = 212$ $[kg]$ : mass of the platform and mass of the cables found in previous sections

- For the torsion, the friction on the walls are neglected. This opens a discussion on whether a bearing is necessary to enforce this assumption but normally not since the casing is included in the slewing ring.

- $F_{load}$ is the axial load: in its calculation the vertical acceleration is neglected as it is small compared to $g = 9.81$ $[m/s^2]$

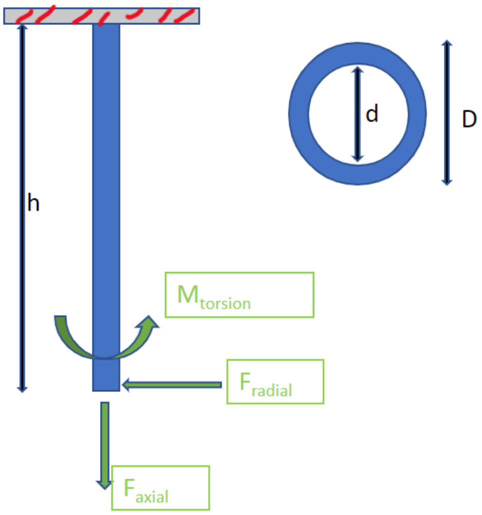


Figure 7: Schematic of the efforts on the slewing ring

**Calculations : Tension**

The axial load comes from the platform and the piece (cables are neglected):

$$\iff F_{load} = (W_{piece} + W_{plat}) \cdot g = 160.982 \text{ [kN]}$$

The area A of the hollow cylinder is : $A = \pi \frac{(D^2 - d^2)}{4}$.

In order to not enter into plasticity (and failure), $\frac{F_{load}}{A}$ must not exceed $\sigma_y$:

$$\sigma_y \geq \frac{F_{load}}{A} \tag{2}$$

$$\iff D_{min} \geq \sqrt{\frac{4F_{load}}{\pi\sigma_y(1 - 1/\phi^2)}} \tag{3}$$

| $\phi$ | 1.5 | 1.2 |
|---|---|---|
| $D_{min}$ | 3.2 [cm] | 4.3 [cm] |

Table 1: Tension - Minimum outer diameter of the vertical cylinder with respect to $\phi$

**Calculations : Torsion**

There is some rotational inertia of the piece, platform and cylinder itself which create a moment on this cylinder. If this moment M is too big, plasticity (and failure) occurs:

$$\tau_y \geq \frac{M_{torsion} \cdot r}{J} \tag{4}$$

where $J$ is the second moment of inertia, M the moment induced by the piece, the platform, etc and $r$ the radius of the cylinder. Now, since plasticity occurs where $r$ is at its maximum value , $r = D/2$. $J$ is equal for a hollow cylinder to $\frac{\pi}{32}(D^4 - d^4)$.
$M = \sum_i I \cdot \dot{\alpha}$ where $\dot{\alpha}$ is the angular acceleration and $I$ the moment of inertia:

- $I_{cylinder} = \frac{1}{8}m(D^2 + d^2) = \dfrac{\pi \rho h}{8}(D^4 - d^4)$
- $I_{platform} = \frac{1}{12}m_{plat}(w^2 + d^2)$ : Using w = 1.5 [m], d = 3 [m] and $m_{plat} = 1410$ $[kg]$. Thus, $I_{platform} = 1321.875$ $[kg/m^2]$.
- $I_{piece}$ : the biggest part to lift are a pair of wings of a total mass of 15 t and with dimensions 34 m over 6 m. The shape of the wing is approximately a rectangle. Thus, its inertia is : $\frac{1}{12}m(w^2 + d^2) = 1490000$ $[kg/m^2]$. This is a huge value comparing to the platform.

Collecting all the moments of inertia:

$$\tau_y \geq \frac{(\frac{\pi \rho h}{8} D^4(1 - 1/\phi^4) + 1518 + 1490000) \cdot D/2 \cdot \dot{\alpha}}{\frac{\pi}{32} D^4 \cdot (1 - 1/\phi^4)} \tag{5}$$

This is a non-linear inequality but can be solved numerically. There is a range of D which fit the inequality (5) depending greatly on $\dot{\alpha}$ and $\phi$:
In table 2, $\dot{\alpha} = 0.008$ $[rad/s^2]$ :

| $\phi$ | 1.5 | 1.2 |
|---|---|---|
| $D_{min}$ | 8 [cm] | 9.3 [cm] |

Table 2: Torsion - Minimum diameter of the vertical cylinder with respect to $\phi$

**Calculations : Bending**

The trolley is moving in the $x$ and $y$ direction. The maximum acceleration/deceleration of the trolley is 0.2 $[m/s^2]$. By action-reaction by accelerating the trolley, the platform via the cables will exert a force on the cylinder. We assumed that it is exerted on the low part of the cylinder. D has to be chosen such that bending will not affect the cylinder.
The vertical column behaves as a built-in beam where the attachments is on the slewing ring and the force exerted on the other end as shown on figure 7.

To avoid bending :

$$\sigma_y \geq \frac{F_{radial} \cdot h \cdot y}{I} \tag{6}$$

where $y = D/2$ and $M = F \cdot h$. F is the force exerted during x/y acceleration/deceleration : $F = 0.2 \cdot (w_{platform} + w_{piece}) = 3.282$ $[kN]$.
$I$ is the second moment of area : $I_x = \frac{\pi}{64} D^4(1 - 1/\phi^4)$.

$$D_{min} \geq \left(\frac{F \cdot h}{\frac{\pi}{32}(1 - 1/\phi^4)\sigma_y}\right)^{1/3} \tag{7}$$

As in the previous results, $D$ depends on $\phi$:

| $\phi$ | 1.5 | 1.2 |
|---|---|---|
| $D_{min}$ | 6.1 [cm] | 7.1 [cm] |

Table 3: Bending - Minimum diameter of the vertical cylinder with respect to $\phi$

To sum up, efforts in tension, torsion and bending have been studied for the vertical cylinder. To avoid plasticity and failure, the minimum diameter has to be above in the order of 10 [cm]. In reality, this is always respected as the cylinder will adapt to the slewing ring. Those rings have diameters from 30 to 100 cm which is well above the minimum D. Note that the results depend on the parameter $\phi$. Furthermore, if the diameter gets too small, this might involve problems for the torque transmitted by the motor.

### 3.5 Slewing ring selection

In order to choose a slewing ring, it is useful to enumerate the various constraints :

1. Tension : $F_{load} = 160,982 \simeq 161[kN]$ : this force takes into account the weight of the piece and the platform. The weight of the vertical column is not taken into account as it depends on its geometry which in turn is determined by the slewing ring chosen. Once, the slewing ring is chosen a new $F_{load}$ will be calculated.

2. Torsion : $M_{torsion} \simeq I_{piece} \cdot \dot{\alpha} = 11.92\ [kNm]$ (the moment of inertia of the platform and the slewing ring are negligible compared to the piece)

3. Bending : $M_{bending} = F_{perpendicular} \cdot h = 3.282 \cdot 2 = 6.6564\ [kNm]$

$M_{torsion}$ is the torsion that is transmitted via the gear of the slewing ring. But, a shock factor of 1.2 is taken into account : $M_{gear} = M_{torsion} \cdot 1.2 = 14.304\ [kNm]$.

A lot of catalogues reference slew rings. Unfortunately, an expert should be consultant for the specific choice for the part. In order to still dimension the rest of the trolley, we will take as first version a slewing ring from this catalogue from TGB [1] which suits the constraints for transmitted torque and axial tension. The slewing ring chosen is showed on figure 8 and the main data are showed in table 4

| | |
|---|---|
| Maximal torque | 30.5 [kNm] |
| Axial static load | 1598 [kN] |
| Axial dynamic load | 384 [kN] |
| Mass | 118.54 [kg] |
| Outer diameter | 672 [mm] |
| Inner diameter | 432 [mm] |
| Height | 123 [mm] |

Table 4: Slewing ring : main propreties and dimensions

### 3.6 Final vertical cylinder dimensioning

Now that the slewing ring dimensions are known, the cylinder dimensions can be chosen. Its outer $D$ and inner diameter $d$ should be between 432 [mm] and 672[mm] in order to attach the cylinder to the slewing ring.

The main dimensions for the cylinder or displayed in table 5.

| | |
|---|---|
| $\phi$ | 1.2 [-] |
| Outer diameter | 540 [mm] |
| Inner diameter | 450 [mm] |
| Height | 1500 [mm] |
| Mass | 1091.67 [kg] |
| Total mass (cylinder + ring) | 1210 [kg] |

Table 5: Vertical cylinder: main dimensions

Knowing the mass of the vertical column :

$$F_{load} = (w_{piece} + w_{platform} + w_{column}) \cdot g = 172.852 \text{ [kN]}$$

This load is still acceptable for the slewing ring chosen.

[1] https://www.tgb-group.com/en/slewing-rings-catalogue/thank-you-slewing-rings-catalogue-download/

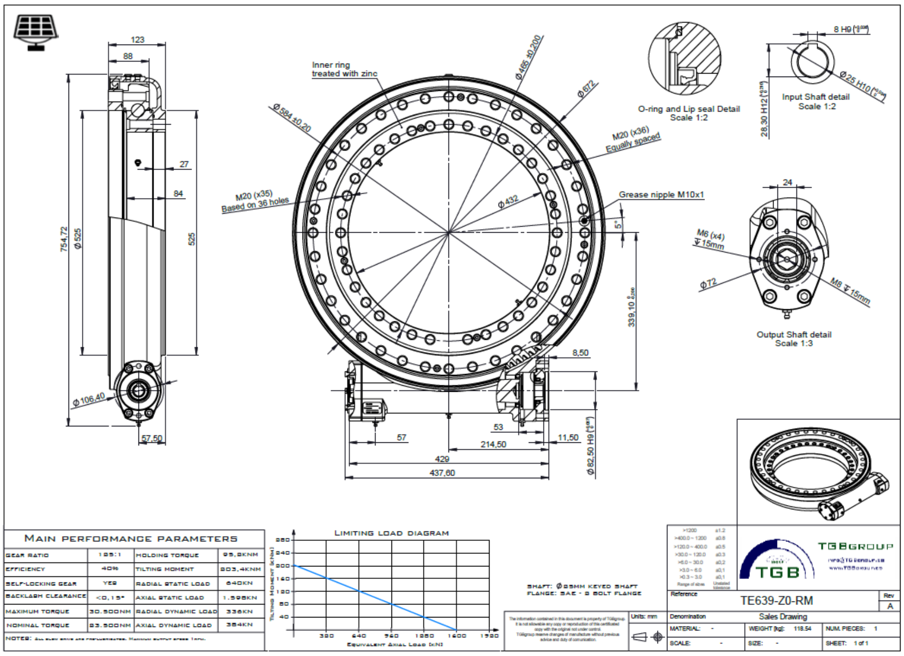


Figure 8: Chosen slewing ring [20]

## 3.7 Trolley

The trolley, which is supported by the two parallel main beams also supports everything that is below (Slewing ring with vertical cylinder, the cables, the platform and the load). We should not forget that there will also be all sets of mechanical machinery (motor, gears, rack and pinion, ...). In fact the design of the trolley's supporting part looks a lot like what has been done for the platform.

**Assumptions**

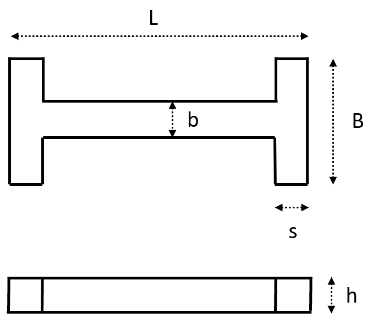


Figure 9: Schematic of the Trolley + notations

- $\gamma = 2$ : We chose a value for the security factor of 2. [10]
- We assumed that the maximum weight (sum of the weight of all the elements below) will be applied at one single point in the middle of the trolley.
- As a material we chose A36 steel with:
  - $\rho = 7860$ [kg/m$^3$]
  - $\sigma_y = 360$ [MPa]
- The design will be made for a rectangular section (just like what we did for the platform) with dimensions $h, b, L$, see figure 9. So the inertia of the section will be $I = \frac{bh^3}{12}$
- Shear stress and axial loading is considered very small compared to the stress induced by the bending moment

**Calculations**

The calculations are exactly the same as for the platform, so we can find the height with the following formula found previously:

$$h > \sqrt{\frac{3\gamma FL}{2b\sigma_y}}$$

And also

$$W_{Trolley} = \rho \cdot (bhL + 2(B-b)hs) \tag{8}$$

and if we fix the values of $L = 2m$, $B = 3m$, $s = 0.3m$ and $b = 1m$, we get:

$$h = 0.06 \quad m$$
$$W_{Trolley} = 1510 \quad kg$$

So in the end if we compute all the weights together and add a bit of free room to count the weight of additional equipment we come out with a weight of $W_{total} = 21.6\,tons$

# 4 Beam dimensioning

The dimensioning of the main beam (50,25m length) is a kind of iteration of some calculation. First, we did preliminary calculations, using some well known profiles (HEA, HEB...) on a software[2]. We directly saw that these profiles could not do the job. We also saw that the deflection (displacement at the center of the beam) was a bigger problem than the internal stress due to bending. So first, let us define a material with a high Young's modulus, to decrease the displacement.

## 4.1 Choice of steel

As we know that the beam has to be rigid enough to avoid a large displacement, we have to look for a high Young's Modulus. Furthermore, we will see that the beam, due to the length, has a big volume. We have to decrease the density, and also look for a material that is not too expensive.

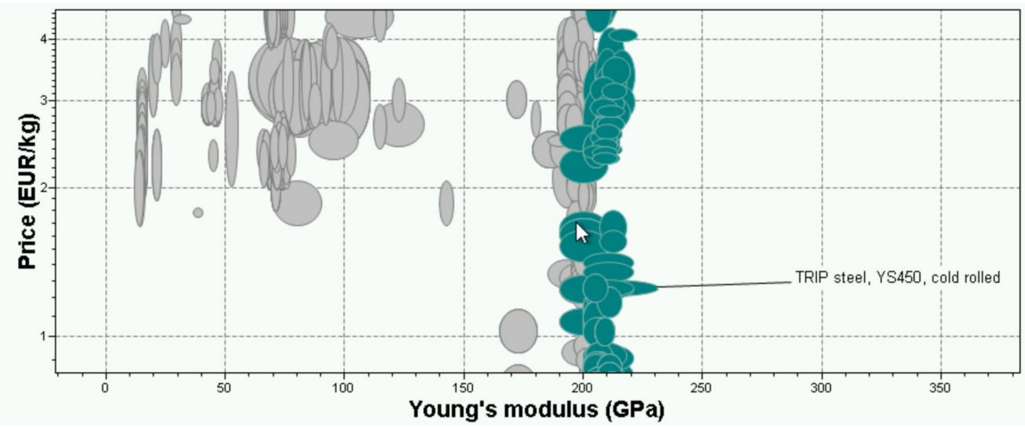


Figure 10: Graph of different material, regarding price and Young Modulus (log scale & linear scale)

Thanks to *Granta EduPack*, we choose TRIP steel, YS450, cold rolled, wich is a common material for longitudinal beams, and sometimes safety component[3]. This material has a quite high Young's modulus, common density for steel, high yield strength. Alloys steel have approximately the same density, this is the reason why density is not a criteria. We choose mean values, except for Young's modulus where we chose a higher value than the mean. These values will be be used in next sections.

| **TRIP Steel YS450 cold rolled** | **Min** | **Max** | **Chosen value** |
|---|---|---|---|
| Density $\rho$ $[kg/m^3]$ | 7800 | 7900 | 7850 |
| Yield strength $\sigma_y$ $[MPa]$ | 450 | 600 | 525 |
| Young modulus $E$ $[GPa]$ | 191 | 231 | 220 |
| Price $[EUR/kg]$ | 1.22 | 1.31 | 1.26 |

[2]We use the software Issd, created by P. Lateur
[3]For example, this material is used in B-pillar reinforcement

## 4.2 Section of the beam

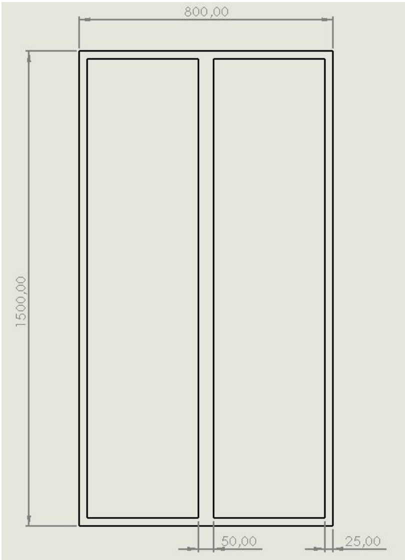


Figure 11: Section of the beam [mm]

Here is the section of the beam. The dimensions are expressed in [mm]. This is 2 rectangles of thickness $t = 25\,mm$ that are fixed/welded side by side. We can observe that the height is quite high to increase inertia. The area of the section of the beam is computed as $A = 1.5 \cdot 0.8 - 2 \cdot (0.35 \cdot 1.45) = 0.185\,m^2$. The volume is then $0.185 \cdot 50.25 = 9.296\,m^3$. The weight of one beam is computed with the density found before : W = 72975.5 kg.
We also need to compute the second moment of area of this section. It will be useful in the calculation of deflection and of the stress inside the beam. This inertia is computed as $I_{x,final} = I_{x,br} - 2 \cdot I_{x,sr}$, where $I_{x,br}$ is the inertia of the big rectangle $I_{x,br} = \frac{bh^3}{12} = \frac{1.5^3 \cdot 0.8}{12} = 0.225\,m^4$

$$
\begin{aligned}
I_{x,sr} &= \int_{0.025}^{0.375} \int_{0.725}^{0.725} y^2 dydx \\
&= \int_{0.025}^{0.375} \left[\frac{y^3}{3}\right]_{0.725}^{0.725} dx \\
&= 0.35 \cdot 0.25405 \\
&= 0.08891\,[m^4]
\end{aligned}
\tag{9}
$$

Total inertia is finally : $I_{x,final} = 0.225 - 2 \cdot 0.08891 = 0.047164\,[m^4]$

## 4.3 Deflection of the beam

We have to consider 2 loads for the beam of 50.25 [m] and section defined before. The load applied on the beam (point load due to the trolley (21.6 tons)) and the weight of the beam (uniform distributed load). The punctual load (for one beam) is 106 [kN], and we assume that the length of the trolley is neglectable compared to the length of the beam. The load due to the weight is $715.89kN$ distributed on the total length, so $q = 729.555/50.25 = 14.246[kN/m]$. The values of the deflection is then :

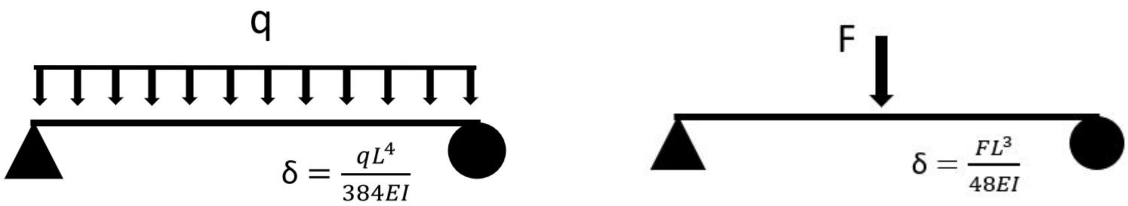


(a) uniform distributed form

(b) ponctual load

Figure 12: Deflection of the meam

$$
\delta_1 = \frac{FL^3}{48EI} = \frac{106 \cdot 10^3 \cdot 50.25^3}{48 \cdot 220 \cdot 10^9 \cdot 0.047164} = 0.027\,[m]
$$

$$
\delta_2 = \frac{5qL^4}{384EI} = \frac{5 \cdot 14.246 \cdot 10^3 \cdot 50.25^4}{384 \cdot 220 \cdot 10^9 \cdot 0.047164} = 0.114\,[m]
$$

The total deflection is 0.141 m. This is a bit less than 0.3 % of the total length of the beam. To obtain these results, we have made the assumption that we are still in the elastic domain so we can sum the 2 computed deflection. We will check that in the next section.

## 4.4 Check of the internal stress

To compute the stress, we have to know the bending moment of these two loads :

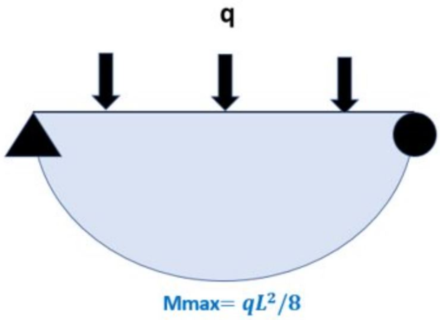


(a) uniform distributed load

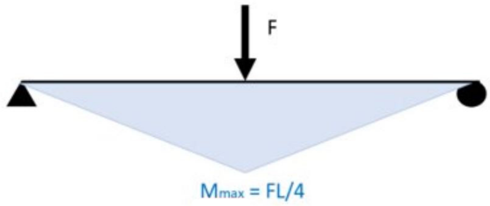


(b) ponctual load

Figure 13: Deflection of the meam

The stress due to the bending moment is : $\sigma = \frac{My}{I}$, where y is h/2 = 0.75 [m], and I the inertia computed before.

$$\sigma = \frac{\left(\frac{qL^2}{8} + \frac{FL}{4}\right) \cdot y}{I}$$

$$\sigma = \frac{\left(\frac{14.246 \cdot 10^3 \cdot 50.25^2}{8} + \frac{106 \cdot 10^3 \cdot 50.25}{4}\right) \cdot 0.75}{0.047164}$$

$$\sigma = 92.678\,[MPa]$$

We see that we are in the elastic domain because $\sigma < \sigma_y \cong 525\ [MPa]$. The summation assumption for deflection and bending moment to compute de stress can be done.

# 5 Rack and pinion selection

The rack and pinion are selected from *Atlanta* catalogue [5]. Following the procedure of selection, the different steps are described :

1. Compute the maximal tangential force to apply on the rack. In order to do so, it is required to know the force needed in order to move the trolley and all the masses hanging below. That force takes into account the friction force to overcome as well as the inertia due to the maximal acceleration at start :

$$F_t = m \cdot (\mu \cdot g + a) \cdot K_S \simeq 11.31\,[kN]\ ,$$

with the friction coefficient assumed to be $\mu = 0.005$, the maximal linear acceleration of the trolley, according to the specifications, $a = 0.3\,[m/s^2]$, and the safety factor on the force $K_S = 1.5$ chosen on the criteria of *Juvinall* [10].

2. The catalogue claims that the condition which has to be satisfied in order to select the rack and pinion is :

$$F_{u,\,permissible} = \frac{F_{u,\,tab}}{K_A \cdot f_n \cdot L \cdot S_B} \geq F_{max}\ ,$$

where $K_A = 1.5$ is the load factor chosen *"for a light shocks drive and medium shocks from the machine to be driven"* according to the manufacturer, $f_n = 3.0$ is the life-time factor for a monthly lubrication (it could be less for a more frequent lubrication but we decided to choose this value though), $L = 1.2$ is the Linear Load Distribution Factor. It is important to notice that the manufacturer uses a safety factor $S_B$ but, since we already applied a safety factor on the force $F_t$, we will not apply a new one again. The manufacturer suggests a safety factor between 1.1 and 1.4, so the value we choose seems a good compromise ($K_S = 1.5$). Finally, $F_{u,\,tab}$ is the maximal feed force that can be exerted on the rack and is provided for each rack.
The minimal $F_{u,\,tab}$ can be computed :

$$F_{u,\,tab} \geq F_t \cdot K_A \cdot f_n \cdot L \simeq 61.08\,[kN]\ .$$

3. The rack can, now, be selected. It is important to notice that all the values of $F_{u,\,tab}$ are not especially available and/or have an adequate corresponding pinion (with the same module as the one of the rack). After that, the number of teeth and the pitch diameter specified have to be respected as well. For the application of the rolling crane, a *High Precision Rack* (HPR) is wanted, according to the *Atlanta* catalogue situated in Appendix A. The latter provides several qualities for that kind of rack and pinion. Choosing a rack and pinion of quality 7 (which is designed for *"Linear Axis with High Requirement for a Smooth Running"*) and a module 6, the material and heat treatment as specified by the manufacturer, as shown on Figure 38. After several tries, the value of $F_{u,\,tab} = 71.5\,[kN]$ and the pinion has to have 21 teeth and a pitch diameter $d = 126\,[mm]$.

4. Once the rack and pinion have been identified their availability has to be checked in the catalogue, as well as their material and their heat treatment. The "final" tables where the rack and pinion have been chosen are provided in Appedix A. The pinion has two possible geometries, with an inner diameter $d_1$ that can be either $75\,[mm]$ or $55\,[mm]$. For the shaft dimensioning, it seemed better to choose the one with an inner diameter $d_1 = 75\,[mm]$, which is a standard shaft diameter as well as a standard bearing bore.

# 6 Motor and reducer selection

In order to select the motor and the reducer, it is required to compute the torque to apply on the pinion in order to start moving the trolley on the rails. As already explained, taking into account the inertia due to the acceleration of the trolley and the other bodies hanging below, the maximal torque required is during the constant acceleration phase :

$$T = F_t \cdot \frac{d}{2} \simeq 712.5\,[N \cdot m]\ ,$$

where $d = 126\,[mm]$ is the pitch diameter of the pinion and $F_t = m \cdot (\mu \cdot g + a) \cdot K_S \simeq 11.31\,[kN]$ was already computed in section 5. From the specifications, it is known that the maximal linear speed of the trolley is $v = 0.3\,[m/s]$, resulting in a angular speed of the pinion of $\omega \simeq 4.762\,[rad/s] \simeq 45.5\,[rpm]$ , so we calculate the power $P = F_t \cdot v \simeq 3.4\,[kW]$

ebitt

**ELECTRICAL PERFORMANCE DATA 50Hz**

| MOTOR TYPE | HOUSING | NOMINAL VALUES Power kW | Power HP | Speed rpm | Current A | Torque Nm | STARTING VALUES Current (Ia/In) Y | Current (Ia/In) Δ | Torque (Ma/Mn) Y | Torque (Ma/Mn) Δ | Breakdown torque ratio | EFFICIENCY η % 4/4 | η % 3/4 | η % 2/4 | Cos 4/4 | J kgm2 | Weight kg | Sound Level dBA |
|---|---|---|---|---|---|---|---|---|---|---|---|---|---|---|---|---|---|---|
| **4 pole 1500 rpm** | | | | | | | | | | | | | | | | | | |
| Q2E71M4C * | aluminum | 0,25 | 1/3 | 1415 | 0,7 | 1,7 | 4,4 | - | 2,3 | - | 3,4 | 68,5 | 68,8 | 68,8 | 0,74 | 0,00095 | 9 | 45 |
| Q2E71M4D * | aluminum | 0,37 | 1/2 | 1415 | 1,1 | 2,5 | 4,4 | - | 2,3 | - | 3,4 | 72,7 | 73,1 | 72,0 | 0,75 | 0,00095 | 8,5 | 45 |
| Q2E80M4B * | aluminum | 0,55 | 3/4 | 1415 | 1,5 | 3,7 | 4,8 | - | 2,8 | - | 3,2 | 77,1 | 77,6 | 76,4 | 0,76 | 0,00205 | 10,5 | 49 |
| Q2E80M4D | aluminum | 0,75 | 1,0 | 1435 | 2 | 5,1 | 5,2 | - | 2,9 | - | 3,2 | 79,6 | 78,9 | 75,3 | 0,7 | 0,00268 | 12 | 49 |
| Q2E90L4C | aluminum | 1,1 | 1,5 | 1430 | 2,5 | 7,4 | 6,7 | - | 2,9 | - | 3,3 | 81,4 | 80,8 | 78,1 | 0,81 | 0,00365 | 18 | 54 |
| Q2E90L4D | aluminum | 1,5 | 2,0 | 1430 | 3,5 | 10,0 | 7,0 | - | 3,2 | - | 3,6 | 82,8 | 82,0 | 79,3 | 0,76 | 0,00365 | 18 | 55 |
| Q2E100L4C | aluminum | 2,2 | 3,0 | 1430 | 5,0 | 14,6 | 7,1 | - | 3,9 | - | 4,2 | 84,3 | 83,8 | 81,2 | 0,77 | 0,00545 | 26 | 56 |
| Q2E100L4D | aluminum | 3,0 | 4,0 | 1440 | 6,4 | 20,0 | 7,1 | - | 3,4 | - | 3,8 | 85,5 | 85,1 | 83,0 | 0,75 | 0,00581 | 26 | 56 |
| Q2E112M4C | aluminum | 4,0 | 5,5 | 1440 | 8,7 | 26,3 | 2,6 | 7,9 | 0,9 | 2,8 | 3,9 | 86,6 | 86,0 | 84,5 | 0,81 | 0,01123 | 31 | 58 |
| Q2E132M4B | aluminum | 5,5 | 7,5 | 1450 | 11,7 | 36,2 | 2,4 | 7,1 | 1,1 | 3,2 | 3,9 | 87,7 | 87,6 | 85,2 | 0,81 | 0,02763 | 54 | 61 |
| Q2E132M4C | aluminum | 7,5 | 10,0 | 1450 | 15,8 | 49,4 | 2,9 | 8,7 | 0,9 | 2,8 | 4,1 | 88,7 | 88,5 | 86,6 | 0,80 | 0,02980 | 57 | 61 |
| Q2E160M4B | aluminum | 11,0 | 15,0 | 1460 | 22,5 | 72,5 | 2,0 | 6,0 | 0,7 | 2,2 | 2,7 | 89,8 | 89,7 | 88,2 | 0,83 | 0,05547 | 76 | 63 |

220/380 V

Figure 14: motor selection : Reference : Motor, 2E112M4C [7]

We select an AC induction motor from *Ebitt motor* [7] catalogue. We will choose a 4 poles induction motor because it can produce the same amount of power at lower rotational speed compared to a 2 poles motor. As we know that, at the end of pinon, the linear velocity of $0.3[m/s]$ is needed which is approximately equal $46[rpm]$. Hence, we select Motor (2E112M4C) which produces a power of $4[kW]$ at $1500[rpm]$ giving a nominal toque of $26.3[N \cdot m]$.

**DIMENSION - B3**

| | | | | Main Dimensions | | | Foot Mounted Motors | | | | | | Shaft | | | | Bearing | | Seal | |
|---|---|---|---|---|---|---|---|---|---|---|---|---|---|---|---|---|---|---|---|---|
| Power (kW) | Number of Poles | Motor Type | Housing Type | AC | L | O | B | A | H | HD | K | C | D(1) | E | GA | F(2) | Drive Side | Non drive Side | Drive Side | Non drive Side |
| 4 | 2 | Q2E100L2DE | Aluminium | 217 | 352,0 | 1*M25 | 140 | 160 | 100 | 241 | 12 | 63 | 28 | 60 | 31 | 8 | 6306-2Z | 6205-2Z | 30*47*7 | 25*40*7 |
| | 2 | Q2E112M2C | Aluminium | 232 | 395,5 | 2*M25 | 140 | 190 | 112 | 261 | 12 | 70 | 28 | 60 | 31 | 8 | 6306-2Z | 6206-2Z | 30*47*7 | 30*47*7 |
| | 4 | Q2E112M4C | Aluminium | 232 | 395,5 | 2*M25 | 140 | 190 | 112 | 261 | 12 | 70 | 28 | 60 | 31 | 8 | 6306-2Z | 6206-2Z | 30*47*7 | 30*47*7 |
| | 6 | Q2E132M6B | Aluminium | 279 | 475,5 | 2*M32 | 178 | 216 | 132 | 314 | 12 | 89 | 38 | 80 | 41 | 10 | 6208-2Z | 6208-2Z | 40*62*10 | 40*62*10 |

Figure 15: motor selection : Reference 2E112M4C[4]

**DIMENSIONS**

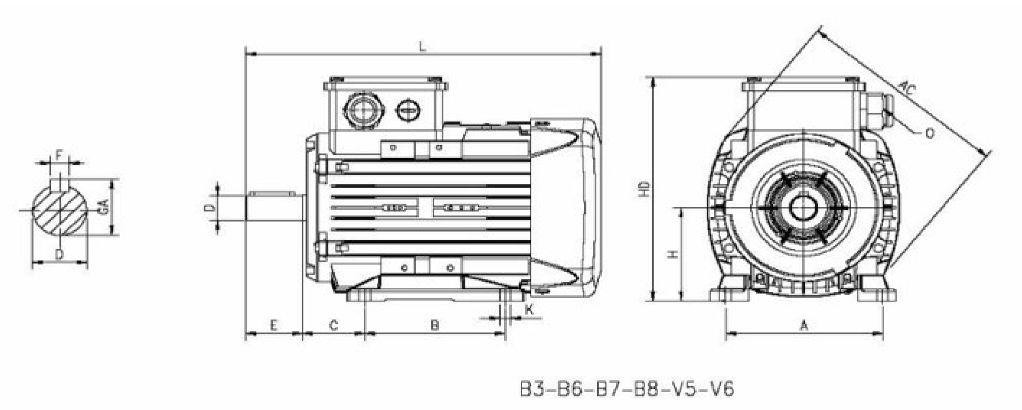


Figure 16: motor detailed image : Reference [4]

Now we have selected the motor according to our requirements, we will see the detail dimensions to check that it is a proper fit for our reducer which we are going to select. Otherwise we change our selection of reducer. Again, from catalogue we can see that the main dimension of output shafts of motor are diameter and length $D = 28\,[mm]$ $L = 395.5\,[mm]$ respectively which can also seen in the figure above.

## 6.1 Reducer

Now we select the reducer based on our requirements. For the selection of the reducer, we are going to use *SESAME* [14] PGL reducer catalogue situated in Appendix B. It will be a planetary gear reducer, with a reduction ratio of 35 in 2 stages. The reduction ratio is calculated with help of motor speed ($1500\,[rpm]$) and the speed required on pinon (around $46\,[rpm]$). We find the maximum reduction ratio for a linear velocity $v = 0.3\,[m/s]$, as mentioned in specifications. Hence we go in the catalogue and select *PGL-180 reducer* for a reduction ratio of 35 and running on nominal speed of $2000[rpm]$.

Figure 17: adjustable coupler

- After we have selected the reducer, we check its dimensions because as we are using motor and reducer from different manufacturing so we need to make sure if both of them can be perfectly mated. This *PGL reducer* uses a dynamic balanced collar mechanism to couple between output shaft of motor and input end of reducer, which helps in maintaining zero slip power transmission at high speeds and also provide adjustability in diameter up to a specific value.

We see that the maximum limit for diameter of input end at reducer side is $50\,[mm]$, where as our output shaft for motor has diameter of $28\,[mm]$ so it means we can perfectly mate these two by just adjusting dynamic balanced collar coupler. The problem that arises now is that output shaft of reducer has diameter of $55\,[mm]$ while our pinon has a bore of of $75\,[mm]$, so we need to design a shaft that has a diameter of $75\,[mm]$ which can provide link between the gear on reducer and and pinon.

| Dimensions | PGL42 | PGL60 | PGL90 | PGL115 | PGL142 | PGL180 |
|---|---|---|---|---|---|---|
| D1 | 50 | 70 | 100 | 130 | 165 | 215 |
| D2 | 3.4 | 5.5 | 6.5 | 8.5 | 10.5 | 13 |
| D3 h6 | 13 | 16 | 22 | 32 | 40 | 55 |
| C1 2 | 46 | 70 | 90 | 115 | 145 | 200 |
| C2 2 | M4x0.7P | M5x0.8P | M6x1.0P | M8x1.25P | M8x1.25P | M12x1.75P |
| C3 2 | ≤8 | ≤14 | ≤19/≤24 | ≤24/≤28 | ≤35 | ≤50 |

Figure 18: reducer Dimension : Reference PGL - 180T [14]

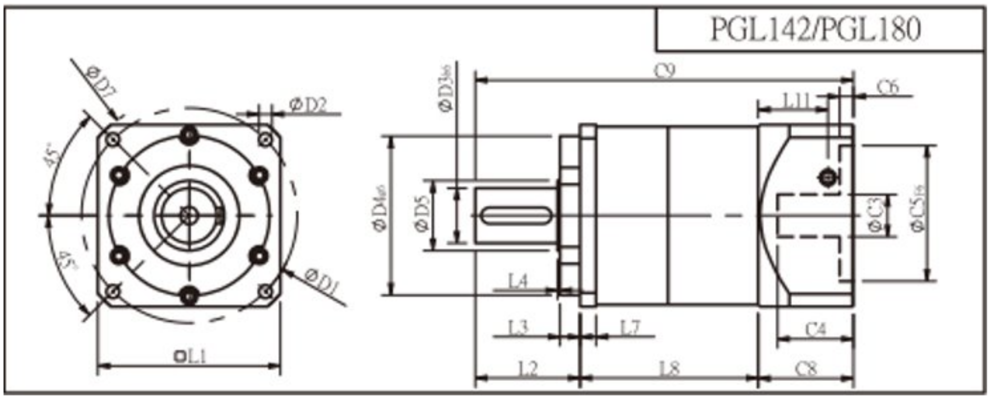


Figure 19: reducer detailed image : Reference PGL [14]

### 6.2 Motor drive unit

Selecting a motor drive unit is very important in this type of problem because we are dealing with a variable speed problem in which the linear velocity varies from $v = 0.0\,[m/s]$ to $0.3[m/s]$. A *variable-frequency drive* (VFD) or *adjustable-frequency drive* (AFD) will be used to control AC motor speed and torque by varying motor input frequency and voltage. The AC electric motor used in a VFD system is usually a three-phase induction motor as we have selected for our application.

## 7 Shaft dimensioning

As already explained in Section 6, the use of an additional gear placed on the output shaft of the reducer is explained by the fact that the shaft on which the pinion will be fixed has to have a $75\,[mm]$ diameter.
For the shaft dimensioning, the first part will focus on the static loading while the fatigue strength will be considered in a second time.

### 7.1 Assumptions

- the torque is constant on the shaft : $T = 712.5\,[N \cdot m]$,
- the diameter of the gear is $150\,[mm]$,
- the geometrical dimensions are the ones presented on Figure 20,
- the weight of the shaft, the gear, the bearings and the pinions are neglected,
- there is no shear force
- the torsion is only due to the torque transmission from the reducer to the pinion

- the stress concentration factors for the bending and the torsion are, respectively, $K_{t,M} \simeq 1.35$ and $K_{t,T} \simeq 1.1$, which are the values from *Juvinall*, Chapter 4 (Section *Stress Concentration Factors,* $K_t$) [10], for $D/d = 1.01$ and $r/d = 0.1$. However, it will be considered that there is no "shoulder" on the shaft, it is a uniform diameter on the whole length, $d = 75\,[mm]$

## 7.2 Notations

- $V$ corresponds to a vertical force while $H$ correspond to an horizontal force,
- $M_V$ is the bending moment due to the vertical force $V$ and $M_H$ the bending moment due to the horizontal force $H$,
- the subscripts $B_1$ and $B_2$ correspond to the bearings 1 and 2, as shown on Figure 20 while the subscripts $p$ and $g$ stand for the pinion and the gear,
- $H_p = F_t$ (computed before) is the tangential force on the pinion and $H_g$ is the tangential force on the gear,
- $V_p = H_p \cdot \tan(20°)$ considering the usual pressure angle of 20° and $V_g = H_g \cdot \tan(20°)$.

## 7.3 Static stresses

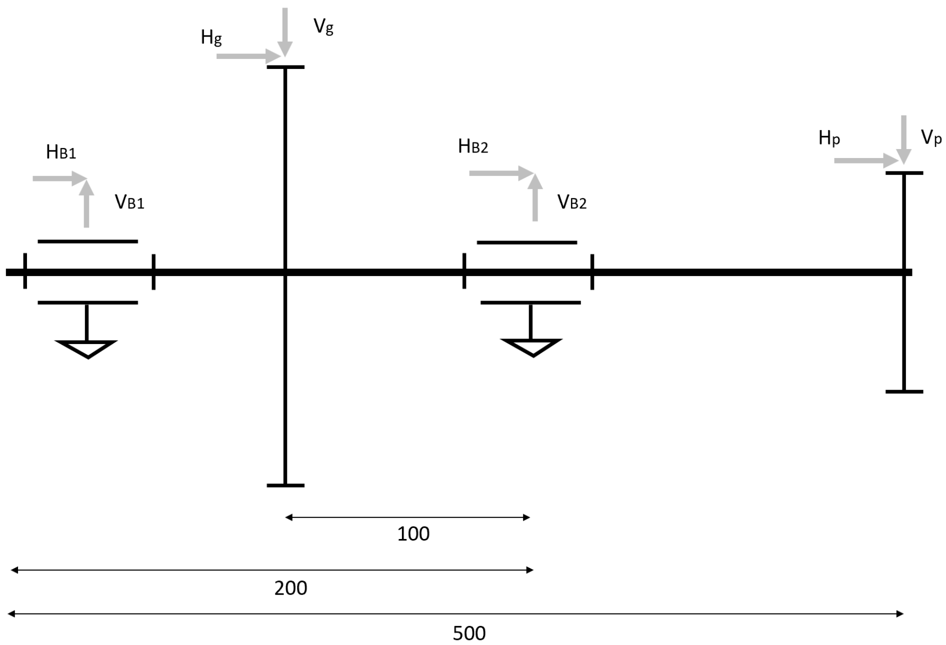


Figure 20: Shaft dimensioning in static

In order to compute the static stresses, the following equations have to be solved :

$$\begin{cases} \sum V &= 0 &= V_{B_1} + V_{B_2} + V_p + V_g \\ \sum M_V &= 0 &= 0.1 \cdot V_g + 0.2 \cdot V_{B_2} + 0.5 \cdot V_p \\ \sum H &= 0 &= H_{B_1} + H_{B_2} + H_p + H_g \\ \sum M_H &= 0 &= 0.1 \cdot H_g + 0.2 \cdot H_{B_2} + 0.5 \cdot H_p \end{cases}$$

Solving that system of equations, we obtain :

$$\begin{cases} V_{B_1} &= -4.4515 & [kN] \\ V_{B_2} &= 12.0285 & [kN] \\ H_{B_1} &= 12.2155 & [kN] \\ H_{B_2} &= -33.0245 & [kN] \end{cases}$$

## 7.4 Internal loads diagram and equivalent static stresses

Diagrams of the vertical and horizontal loads on the shaft as well as the bending moments diagrams show that the critical locus is at the position of the second bearing, as shown on the Figures 21 and 22.

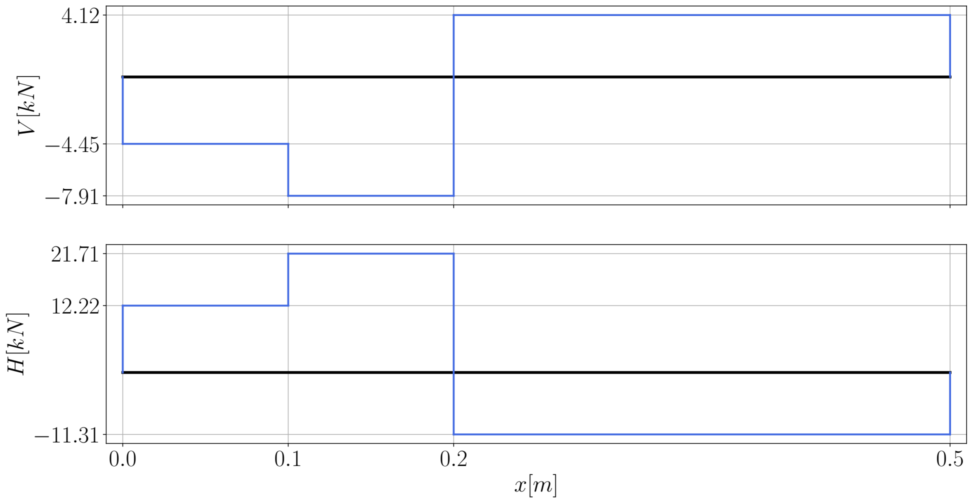


Figure 21: Internal loads diagrams : Forces

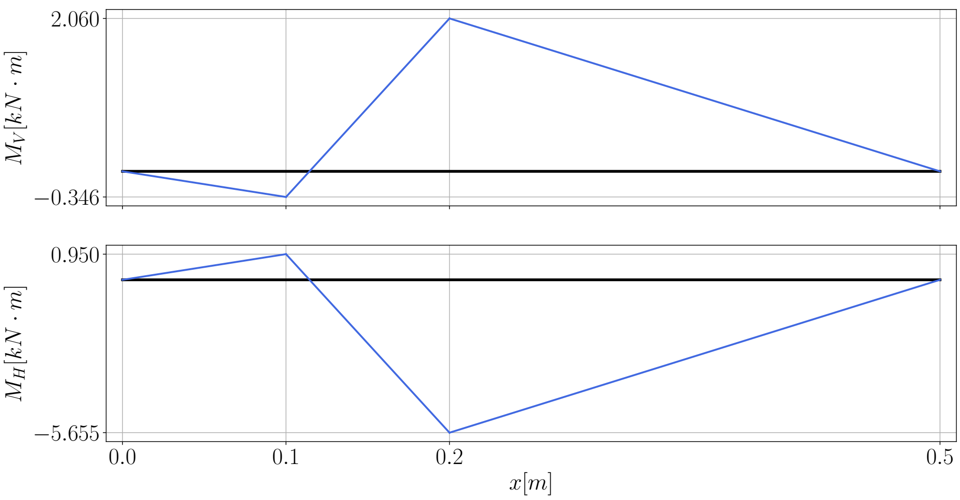


Figure 22: Internal loads diagrams : Bending moments

Applying the stress concentration factors formulated in the assumptions, we have that the maximal static stresses at that critical locus are given by :

$$\begin{cases} \sigma_{nom} & = \frac{32 \cdot M_{max}}{\pi \cdot d^3} & \simeq 145.35 & [MPa] \\ \tau_{nom} & = \frac{16 \cdot T_{max}}{pi \cdot d^3} & \simeq 8.61 & [MPa] \end{cases}$$

where $M_{max} = \sqrt{M_{V_{B_2}}^2 + M_{H_{B_2}}^2} \simeq 6.02\,[kN \cdot m]$.
Taking now the stress concentration factors into account :

$$\begin{cases} \sigma_{max} & = \frac{32 \cdot M_{max}}{\pi \cdot d^3} \cdot K_{t,\,M} & \simeq & 196.23 & [MPa] \\ \tau_{max} & = \frac{16 \cdot T_{max}}{pi \cdot d^3} \cdot K_{t,\,T} & \simeq & 9.47 & [MPa] \end{cases}$$

Thus, the shaft material should be chosen such that :

$$\sigma_{eq} = \sqrt{\sigma_{max}^2 + 3 \cdot \tau_{max}^2} \simeq 196.80\,[MPa]\,.$$

The material which will be chosen in order to manufacture that shaft will thus be : *Carbon and alloy steel 1018 A* with $\sigma_y = 221\,[MPa]$ and $\sigma_u = 341\,[MPa]$ [10].

### 7.5 Fatigue strength

For the fatigue, the equivalent alternating bending stress $\sigma_{ea}$ is assumed to be only due to bending while the equivalent mean bending stress $\sigma_{em}$ (on a cycle) is assumed to be only due to torsion. That is, $\sigma_{ea} = \sigma_a = \sigma_{max}$ and $\sigma_{em} = \tau_m = \tau_{max}$ (on a cycle). The fatigue strength will be made for a $10^3$-cycle strength since the shaft will not undergo long cycles on its life (since it is only required for the translation of the trolley in the width of the hangar). According to the *Juvinall* procedure described in *Section 8 - Influence of Surface and Size on Fatigue Strength* [10] :

$$\sigma_n = 0.9 \cdot 0.8 \cdot \sigma_u = 245.52\,[MPa] \ ,$$

for the material chosen (*Carbon and alloy steel 1018 A*). As shown on Figure 23, the material allows to sustain the fatigue strength, since the point $(\sigma_{em}, \sigma_{ea})$ (red point on the Figure) is below the two lines.

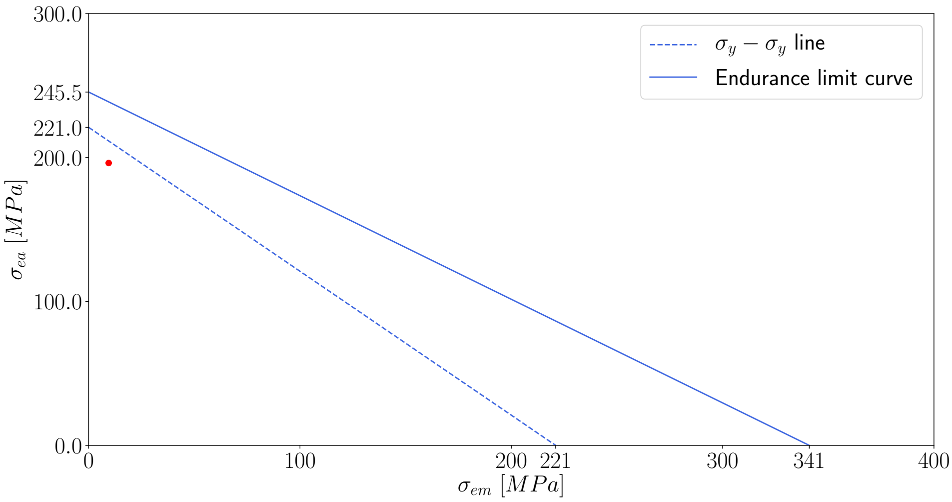


Figure 23: Fatigue strength diagram

## 8 Bearings selection

Using the SKF [18] procedure (described on the manufacturer website), the required bearings can be selected. Since the loading is mainly axial, ball bearings will be selected in the sorts of bearings. Both types of dimensioning will be done to ensure no failure.

### 8.1 Static load dimensioning

This kind of dimensioning has to be done for *"bearings running under very low speeds or which are used under stationary conditions, very bad lubrication conditions or where occasional peak loads occur"*. The *basic static load rating* $C_0$ for this application needs to be computed for the selection of the bearings.

Assuming there is no axial load (since it is mainly radial), the *equivalent static bearing load* $P_0$ can be computed and, after that, choosing the static safety coefficient $s_0 = 2$ (for high certainty and permanent deformation unwanted, according to the SKF procedure).

$$P_0 = X_0 \cdot F_r + Y_0 \cdot F_a \ ,$$

with $Y_0 = 0$, the axial load factor for the bearing, and $X_0 = 1$, the radial load factor for the bearing. Thus, $P_0 = F_r = \sqrt{V_{B_2}^2 + H_{B_2}^2} \simeq 35.15\,[kN]$. Leading to $C_0 = s_0 \cdot P_0 \simeq 70.3\,[kN]$.

### 8.2 Rating life dimensioning

Rating life is the number of operating hours (or revolutions) of the bearing before failure due to fatigue. $L_r$ is the rating life where $r$ [%] of bearings of that type would statically have failures. For example, a life rating of $L_{10}$ corresponds to the number of revolutions after which 90% of the same type of bearings still work.
For the shaft actuating the pinion, $L_{h10} = 25\,000$ $[h]$ (for *"Machines for use 8 hours a day, but not always fully utilized: gear drives for general purposes, electric motors or for industrial use, rotary crushers"*). After

that, it is required to compute $L_{h10} = \frac{10^6}{60 \cdot \omega} \cdot L_{10}$, where $\omega = 46\,[rpm]$ is the rotational speed of the shaft. $L_{10} = \frac{60}{\omega \cdot 10^6} \cdot L_{h10} \simeq 1.5$.
The final step requires to compute the basic dynamic load rating C, given by :

$$L_{10} = \left(\frac{C}{P}\right)^p \text{ , with } \; p = 3 \text{ for ball bearings.}$$

where $P$ is the equivalent dynamic bearing load and, in this case, $P = P_0 \simeq 35.15\,[kN]$. Which gives : $C = L_{10}^{1/p} \cdot P \simeq 40.3\,[kN]$.

### 8.3 Selection in the catalogue

Knowing the type of bearing, the bore (which corresponds to the 75 $[mm]$ diameter of the shaft), the bearing selected must have its $C_0$ and $C$ values lower than the ones previously computed. The selected bearing is shown on Figure 42 in Appendix C. The main dimensions are the external diameter $D = 160.0\,[mm]$ and the width $B = 37.0\,[mm]$.

## 9 Rollers

Last part of dimensioning is about rollers. We need a set of rollers for the X-translation, along the length of the hangar, and the Y-translation, along the width of the hangar.

**X-Translation** : The rollers for the X-translation have to be able to lift the totality of the system. This includes both beams, the trolley, the lifting up system and the piece to lift. The total mass of these items is around 170t as seen in table One critical case is the configuration where the heaviest place is lifted in one extremity of the crane. As a security, we assumed that rollers on one side of the crane have to be able to carry this maximum mass. To do so, we chose rollers from DEMAG [6] with the following specification:

Figure 24: Rollers DWS 630 [6]

- **Reference :** DEMAG, DWS 630 [6]
- **Numbers of rollers per side :** 3
- **Roller lifting capacity :** 60t
- **Roller diameter :** 630mm
- **Roller mass :** 310kg

**Y-Translation :** The rollers must be able to lift the trolley, in addition of all what is situated below it. The maximum mass is then 20t. But in contrary to the rollers for the X-translation, this mass is well distributed between four rollers, two on each beam. Once again, we use rollers from DEMAG [6] with the following specification:


Figure 25: Rollers DRS 160 [6]

- **Reference :** DEMAG, DRS 160 [6]
- **Numbers of rollers :** 4
- **Roller lifting capacity :** 7t
- **Roller diameter :** 160mm
- **Roller mass :** 18.3kg

# 10 Sensors

## 10.1 Positioning

In order to be able to position the crane and the platform at any time in the hangar, we decided to use laser distance sensors with the following specification :

**Z-Position :**
Maximum distance to measure : 15m
Laser range : 30m
Repeatability : 0.5mm

**Y-Position :**
Maximum distance to measure : 50m
Laser range : 50m
Repeatability : 0.25mm

**X-Position :**
Maximum distance to measure : 200m
Laser range : 0.2-300m
Repeatability : 2mm

Figure 26: Z-Position Laser [17]

Reference : SICK, DL35-B15552

Figure 27: Y-Position Laser [16]

Reference : SICK, DL50-N2225

Figure 28: X-Position Laser [15]

Reference : SICK, DL100-23AA2101

## 10.2 Overload protection

Next sensor is about preventing overloading. This can be problematic for many reason, as being against regulation, but it can as well stress and damage equipment and put workers in direct danger. In order to achieve this protection, we decided to use load pins. We can replace pins in sheaves with load pins and, after calibration, will be able to measure the mass that the crane is lifting. The pins from SENSY [13] will ensure that the crane do not lift beyond its rated capacity. It has the following specification :

Figure 29: Load pin [13]

- **Reference :** AXES DYNAMOMETRIQUES STANDARD 5300-E [13]
- **Numbers of pins :** 2
- **Lift capacity :** 10t
- **Diameter :** 65mm

## 10.3 Runway alignment

We need as well to assure the runway alignment of the crane. Runaway misalignment can cause racking, skewing, or binding that can results in excessive stress of the beams, but will most commonly cause extensive wheel wear. To assure alignment, we will place two laser sensors that will measure the distance between the crane and the support as shown in figure 30.

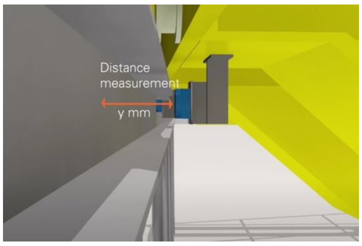


Figure 30: Sensor measurement [12]

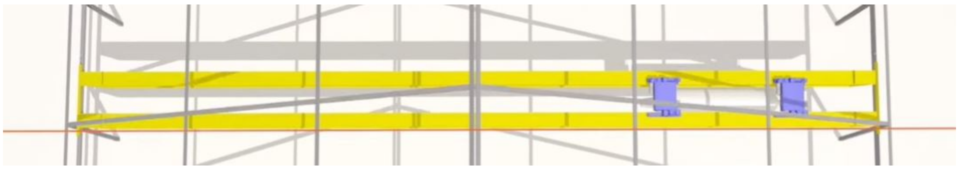

Figure 31: Bridge alignment [12]

Precision sensor from KEYENCE [9] matches our needs and has the following specification :


Figure 32: Precision Sensor [9]

- **Reference :** KEYENCE, LK-H080
- **Reference distance :** 80mm
- **Measuring range :** $\pm 18mm$
- **Repeatability :** $1\mu m$

## 10.4 Speed control

Another set of sensor would be to control the speed of the crane in order to avoid any collision with one end of the hangar. The goal is to define 3 distinct zones where a maximum speed is defined, as shown in figure 33. In order to achieve this goal, we use a limit switch. A limit switch is bonded with the crane and will make contact with a target situated at one place of the hangar, as shown in figure 35. It will rotate the switch and adjust the speed of the crane according to the zone it is located.


Figure 33: Zones

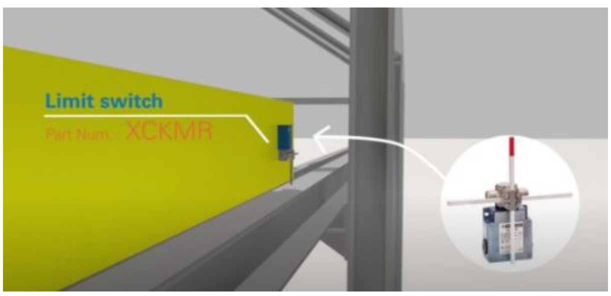


Figure 34: Limit switch 1 [12]

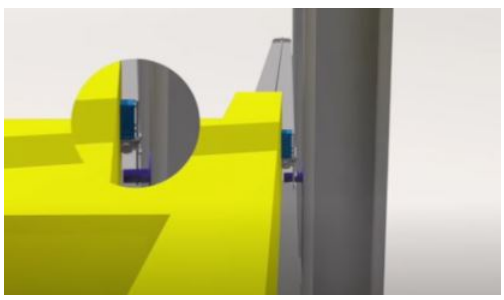

Figure 35: Limit switch 2 [12]

Reference : Telemecanique Sensor, XCKMR44D1H29 [11]

## 10.5 Sway control system

Last sensor is an anti sway control system. Eliminating sway is important when operating with a crane, as undesirable motion can result in accident, and lower productivity. It basically works in two steps :

- **Estimate and calculate load swing :** A smart camera placed under the trolley will use a reflective target on the platform in order to compute the load swing.

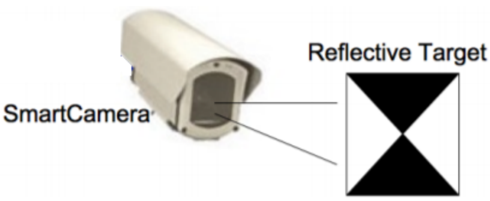


Figure 36: Smart camera [19]

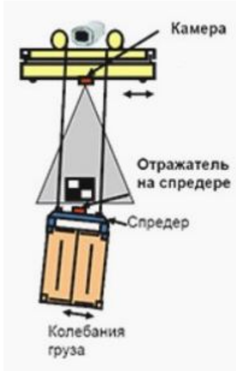


Figure 37: Anti sway system [8]

- **Adjust crane motion :** The anti sway software will translate the swing into carefully timed acceleration directly transmitted to the PLC of the crane.

This system will allow to work safely and more efficiently.
Reference : SmartCrane, Anti Sway Crane Control [19].

# 11 Conclusion

To wrap up, we now have a better idea of the dimensions that our product will have. It is clear that we still have some things to improve or optimize. We decided not to dimension every little part of the machine in the context of this course as this would have been a very big part of work and it would not have fit in this report of twenty pages. Even with our limitations, we are exceeding the maximum number, but still, as there were a lot of things to say, we figured that exceeding a little bit the twenty pages would not be a big problem. We also tried to have the dimensioning of different kind of parts (static elements like the beam, shafts, cables, ...) to avoid redoing the same calculations all over again, which would not be very interesting in the context of the project.

# A Appendix : Rack and pinion selection

ATLANTA — Rack and Pinion Drive – Calculation and Selection – Module 6 – Straight Tooth System

| Rack | | UHPR | HPR | | BR | | | |
|---|---|---|---|---|---|---|---|---|
| Quality | | 4 | 6 | 7 | 9 | | 10 | |
| Rack | Material | C45 | C45 | C45 | C45 | | C45 | |
| | Heat Treatment | Ind. Hardened | Induction Hardened | | Soft | | Induction Hardened | |
| Pinion | Material | 16MnCr5 | 16MnCr5 | 16MnCr5 | 16MnCr5 | C45 | 16MnCr5 | C45 |
| | Heat Treatment | Case Hardened | Case Hardened | Case Hardened | Case Hardened | Soft | Case Hardened | Ind. Hardened |
| No. of Pinion Teeth 1) | Pitch Circle Dia. | Maximum Feed Force | | | | | | |
| 12 | 72 mm | 27.5 kN | 27.5 kN | 27.5 kN | 7.5 kN | 3.0 kN | 25.5 kN | 15.0 kN |
| 13 | 78 mm | 33.5 kN | 33.5 kN | 33.5 kN | 8.0 kN | 3.5 kN | 30.0 kN | 17.5 kN |
| 14 | 84 mm | 41.5 kN | 41.5 kN | 41.5 kN | 8.5 kN | 4.0 kN | 34.5 kN | 20.0 kN |
| 15 | 90 mm | 46.0 kN | 45.5 kN | 45.5 kN | 9.0 kN | 4.5 kN | 38.0 kN | 22.5 kN |
| 16 | 96 mm | 50.5 kN | 50.5 kN | 50.5 kN | 10.0 kN | 5.0 kN | 40.5 kN | 25.0 kN |
| 17 | 102 mm | 56.5 kN | 56.5 kN | 56.5 kN | 11.5 kN | 6.0 kN | 43.5 kN | 27.5 kN |
| 18 | 108 mm | 61.0 kN | 61.0 kN | 61.0 kN | 12.5 kN | 7.0 kN | 46.0 kN | 30.0 kN |
| 19 | 114 mm | 64.5 kN | 64.5 kN | 64.5 kN | 13.0 kN | 7.5 kN | 48.5 kN | 32.5 kN |
| 20 | 120 mm | 68.0 kN | 68.0 kN | 68.0 kN | 14.0 kN | 8.0 kN | 51.0 kN | 34.5 kN |
| 21 | 126 mm | 71.5 kN | 71.5 kN | 71.5 kN | 14.5 kN | 8.5 kN | 53.5 kN | 37.0 kN |
| 22 | 132 mm | 75.5 kN | 75.0 kN | 75.0 kN | 15.5 kN | 9.0 kN | 56.0 kN | 39.5 kN |
| 23 | 138 mm | 79.0 kN | 79.0 kN | 78.5 kN | 16.0 kN | 9.5 kN | 58.5 kN | 42.0 kN |
| 24 | 144 mm | 82.5 kN | 82.5 kN | 82.5 kN | 17.0 kN | 10.5 kN | 61.0 kN | 44.0 kN |
| 25 | 150 mm | 86.0 kN | 86.0 kN | 86.0 kN | 17.5 kN | 11.0 kN | 61.5 kN | 46.5 kN |
| 26 | 156 mm | 87.5 kN | 87.5 kN | 87.5 kN | 18.5 kN | 11.5 kN | 62.0 kN | 49.0 kN |
| 27 | 162 mm | 88.0 kN | 87.5 kN | 87.5 kN | 19.0 kN | 12.0 kN | 62.0 kN | 50.0 kN |
| 28 | 168 mm | 88.5 kN | 88.0 kN | 88.0 kN | 20.0 kN | 12.5 kN | 62.5 kN | 50.0 kN |
| 29 | 174 mm | 88.5 kN | 88.5 kN | 88.5 kN | 20.5 kN | 13.0 kN | 62.5 kN | 50.5 kN |
| 30 | 180 mm | 89.0 kN | 89.0 kN | 89.0 kN | 21.5 kN | 13.5 kN | 63.0 kN | 50.5 kN |

1) Check availability (chapter ZB)

**Maximum permissible feed forces – description see page ZB-36**

Figure 38: Rack and pinion selection chart

ATLANTA — **HPR Racks Module 2–8**

**ATLANTA-Quality 7**

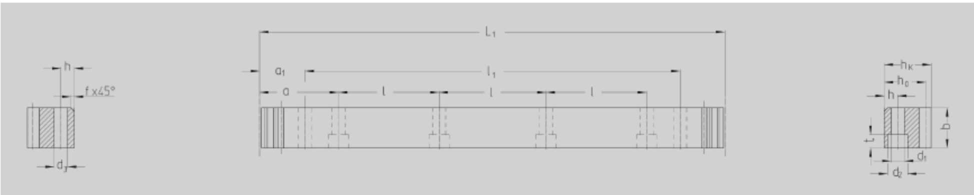


| Order Code | Module | $L_1$ | N° of Teeth | b | $h_k$ | $h_0$ | f | a | l | N° of Holes | h | $d_1$ | $d_2$ | t | $a_1$ | $l_1$ | $d_3$ | kg |
|---|---|---|---|---|---|---|---|---|---|---|---|---|---|---|---|---|---|---|
| **28 20 107** | 2 | 1005.3 | 160 | 24 | 24 | 22 | 2 | 62.8 | 125.66 | 8 | 8 | 7 | 11 | 7 | 31.3 | 942.7 | 5.7 | 4.2 |
| **28 30 107** | 3 | 1017.9 | 108 | 29 | 29 | 26 | 2 | 63.6 | 127.23 | 8 | 9 | 10 | 15 | 9 | 34.4 | 949.1 | 7.7 | 6.0 |
| **28 40 107** | 4 | 1005.3 | 80 | 39 | 39 | 35 | 2 | 62.8 | 125.66 | 8 | 12 | 14 | 20 | 13 | 37.5 | 930.3 | 7.7 | 10.5 |
| **28 50 107** | 5 | 1005.3 | 64 | 49 | 39 | 34 | 2.5 | 62.8 | 125.66 | 8 | 12 | 14 | 20 | 13 | 30.1 | 945.0 | 11.7 | 13.4 |
| **28 60 107** | 6 | 1017.88 | 54 | 59 | 49 | 43 | 2.5 | 63.6 | 127.23 | 8 | 16 | 18 | 26 | 17 | 31.4 | 955.00 | 15.7 | 20.20 |
| **28 80 107** | 8 | 1005.30 | 40 | 79 | 79 | 71 | 2.5 | 62.8 | 125.66 | 8 | 25 | 22 | 33 | 21 | 26.6 | 952.00 | 19.7 | 44.76 |

Figure 39: Rack selection : reference 28 60 107

ATLANTA

Gearwheels with Ground Teeth – Module 5–10

**Straight Tooth System,** with Bore ØH6 and Keyway acc. to DIN 6885

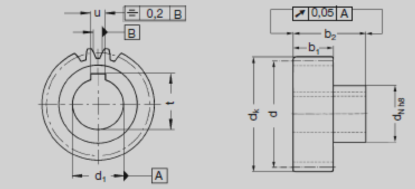

Keyway Middle of Tooth Gap

16MnCr5, 1.7131

Case-Hardened

Gearing Grade
**6 e 25**

| Order Code | Fig. | N° of Teeth z | d | $d_k$ | $d_1^{H6}$ | $d_N$ | $b_1$ | $b_2$ | u | t | kg | Shrink-Disk on Page GH-1 |
|---|---|---|---|---|---|---|---|---|---|---|---|---|
| **Module 5** | | | | | | | | | | | | |
| **24 56 421** | | 21 | 105 | 115 | 45 | 68 | 50 | 85.0 | 14 | 48.8 | 3.7 | 80 80 068 |
| **24 57 421** | | 21 | 105 | 115 | 55 | 80 | 50 | 90.0 | 16 | 59.3 | 3.7 | 80 87 080 |
| **24 56 425** | | 25 | 125 | 135 | 45 | 68 | 50 | 85.0 | 14 | 48.8 | 5.2 | 80 80 068 |
| **24 57 425** | | 25 | 125 | 135 | 55 | 80 | 50 | 90.0 | 16 | 59.3 | 5.1 | 80 87 080 |
| **24 58 425** | | 25 | 125 | 135 | 75 | 110 | 50 | 110.0 | 20 | 80.4 | 4.7 | 80 80 110 |
| **Module 6** | | | | | | | | | | | | |
| **24 67 421** | | 21 | 126 | 138 | 55 | 80 | 60 | 100.0 | 16 | 59.3 | 5.6 | 80 87 080 |
| **24 68 421** | | 21 | 126 | 138 | 75 | 110 | 60 | 120.0 | 20 | 79.9 | 4.7 | 80 80 110 |
| **24 67 425** | | 25 | 150 | 162 | 55 | 80 | 60 | 100.0 | 16 | 59.3 | 8.0 | 80 87 080 |
| **24 68 425** | | 25 | 150 | 162 | 75 | 110 | 60 | 120.0 | 20 | 79.9 | 7.1 | 80 80 110 |
| **Module 8** | | | | | | | | | | | | |
| **24 88 420*** | | 20 | 160 | 176 | 75 | 110 | 80 | 140 | 20 | 79.9 | 12.0 | 80 80 110 |
| **24 89 420*** | | 20 | 160 | 176 | 85 | 125 | 80 | 145 | 22 | 90.4 | 12.1 | 80 80 125 |
| **Module 10** | | | | | | | | | | | | |
| **24 09 620*** | | 20 | 200 | 220 | 85 | 125 | 100 | 165 | 22 | 90.4 | 23 | 80 80 125 |

* Gearing quality 5 f 23

Figure 40: Pinion selection : reference 24 68 421

# B Appendix : Reducer selection

| | | Stage | Ratio | PGL-42 | PGL-60 / 60T | PGL-90 / 90T | PGL-115 / 115T | PGL-142 / 142T | PGL-180 / 180T | PGL-220 / 220T |
|---|---|---|---|---|---|---|---|---|---|---|
| Nominal Output Torque $T_{2N}$ | N • m | 2 | 15 | 13.8 | 44.2 | 95.2 | 283 | 482 | 1151 | 1670 |
| | | | 20 | 11.9 | 35.9 | 74.6 | 249 | 490 | 1055 | 1574 |
| | | | 25 | 13.8 | 43.0 | 95.2 | 283 | 473 | 1151 | 1670 |
| | | | 30 | 13.8 | 43.0 | 95.2 | 283 | 473 | 1151 | 1670 |
| | | | 35 | 13.8 | 43.0 | 95.2 | 283 | 473 | 1151 | 1670 |
| | | | 40 | 13.8 | 43.0 | 95.2 | 283 | 473 | 1151 | 1670 |
| | | | 45 | 13.8 | 43.0 | 95.2 | 283 | 473 | 1151 | 1670 |
| | | | 50 | 13.8 | 43.0 | 95.2 | 283 | 473 | 1151 | 1670 |
| | | | 60 | 12.5 | 39.4 | 90.9 | 266 | 436 | 1055 | 1574 |
| | | | 70 | 11.9 | 36.0 | 85.6 | 219 | 400 | 1055 | 1574 |
| | | | 80 | 10.9 | 32.4 | 85.0 | 216 | 363 | 860 | 1184 |
| | | | 90 | 9.8 | 28.7 | 80.0 | 210 | 320 | 764 | 1185 |
| | | | 100 | 10.1 | 25.0 | 75.0 | 210 | 320 | 763 | 1184 |
| Emergency Stop Torque $T_{2NOT}$ | N • m | | (3.0 times of Nominal Output Torque) ( * Max. Output Torque $T_{2B}$ =60% of Emergency Stop Torque) | | | | | | | |
| Nominal Input Speed $n_{1N}$ | rpm | 1,2 | 3-100 | 3000 | 3000 | 3000 | 2500 | 2000 | 2000 | 2000 |
| Max. Input Speed $n_{1max}$ | rpm | 1,2 | 3-100 | 6000 | 6000 | 6000 | 5000 | 4000 | 4000 | 4000 |
| Micro Backlash P0 | arcmin | 1 | 3-10 | - | - | - | ≦ 3 | ≦ 3 | ≦ 3 | ≦ 3 |
| | | 2 | 12-100 | - | - | - | ≦ 5 | ≦ 5 | ≦ 5 | ≦ 5 |

Figure 41: reducer : reference PGL - 180T [14]

3.1 Single row angular contact ball bearings
d 65 – 75 mm

3.1

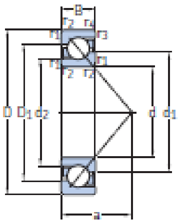


| Principal dimensions | | | Basic load ratings dynamic | static | Fatigue load limit | Speed ratings Reference speed | Limiting speed | Mass | Designations Universally matchable bearing | Basic design / sealed bearing |
|---|---|---|---|---|---|---|---|---|---|---|
| d | D | B | C | $C_0$ | $P_u$ | | | | | |
| mm | | | kN | | kN | r/min | | kg | – | |
| 65 | 120 | 23 | 66,3 | 54 | 2,28 | 6 700 | 6 300 | 1 | – | ▸ 7213 BEP |
| | 120 | 23 | 69,5 | 57 | 2,45 | 6 700 | 6 700 | 1 | ▸ 7213 BECBP | – |
| | 120 | 23 | 69,5 | 57 | 2,45 | 6 700 | 6 700 | 1 | ▸ 7213 BECBY | – |
| | 120 | 23 | 69,5 | 57 | 2,45 | 6 700 | 6 700 | 1 | 7213 BEGAPH | – |
| | 120 | 23 | 69,5 | 57 | 2,45 | 6 700 | 8 500 | 1 | ▸ 7213 BECBM | – |
| | 120 | 23 | 81,5 | 65,5 | 2,8 | 7 000 | 10 000 | 1 | 7213 ACCBM | – |
| | 140 | 33 | 108 | 80 | 3,35 | 6 000 | 5 600 | 2,15 | – | ▸ 7313 BEP |
| | 140 | 33 | 116 | 86,5 | 3,65 | 6 000 | 6 300 | 2,15 | ▸ 7313 BECBP | – |
| | 140 | 33 | 116 | 86,5 | 3,65 | 6 000 | 6 300 | 2,15 | 7313 BECBPH | – |
| | 140 | 33 | 116 | 86,5 | 3,65 | 6 000 | 6 300 | 2,15 | ▸ 7313 BECBY | – |
| | 140 | 33 | 116 | 86,5 | 3,65 | 6 000 | 8 000 | 2,15 | ▸ 7313 BECBM | – |
| | 140 | 33 | 132 | 96,5 | 4,05 | 6 300 | 9 500 | 2,15 | 7313 ACCBM | – |
| 70 | 125 | 24 | 67,6 | 56 | 2,36 | 6 300 | 6 000 | 1,1 | – | ▸ 7214 BEP |
| | 125 | 24 | 72 | 60 | 2,55 | 6 300 | 6 300 | 1,1 | ▸ 7214 BECBP | – |
| | 125 | 24 | 72 | 60 | 2,55 | 6 300 | 6 300 | 1,1 | 7214 BECBPH | – |
| | 125 | 24 | 72 | 60 | 2,55 | 6 300 | 8 000 | 1,1 | ▸ 7214 BECBM | – |
| | 125 | 24 | 75 | 64 | 2,7 | 6 300 | 6 300 | 1,1 | ▸ 7214 BECBY | – |
| | 125 | 24 | 83 | 68 | 2,9 | 6 700 | 10 000 | 1,1 | 7214 ACCBM | – |
| | 150 | 35 | 119 | 90 | 3,65 | 5 600 | 5 300 | 2,65 | – | ▸ 7314 BEP |
| | 150 | 35 | 127 | 98 | 3,9 | 5 600 | 5 600 | 2,65 | ▸ 7314 BECBP | – |
| | 150 | 35 | 127 | 98 | 3,9 | 5 600 | 5 600 | 2,65 | ▸ 7314 BECBPH | – |
| | 150 | 35 | 127 | 98 | 3,9 | 5 600 | 5 600 | 2,65 | ▸ 7314 BECBY | – |
| | 150 | 35 | 127 | 98 | 3,9 | 5 600 | 5 600 | 2,65 | 7314 BEGAPH | – |
| | 150 | 35 | 127 | 98 | 3,9 | 5 600 | 7 000 | 2,65 | ▸ 7314 BECBM | – |
| | 150 | 35 | 143 | 110 | 4,4 | 6 000 | 8 500 | 2,65 | 7314 ACCBM | – |
| 75 | 130 | 25 | 70,2 | 60 | 2,5 | 6 000 | 5 600 | 1,2 | – | ▸ 7215 BEP |
| | 130 | 25 | 73,5 | 65,5 | 2,7 | 6 000 | 6 300 | 1,2 | ▸ 7215 BECBM | – |
| | 130 | 25 | 73,5 | 65,5 | 2,7 | 6 000 | 6 300 | 1,2 | ▸ 7215 BECBP | – |
| | 130 | 25 | 73,5 | 65,5 | 2,7 | 6 000 | 6 300 | 1,2 | 7215 BECBPH | – |
| | 130 | 25 | 76,5 | 69,5 | 2,9 | 6 000 | 6 300 | 1,2 | ▸ 7215 BECBY | – |
| | 160 | 37 | 125 | 98 | 3,8 | 5 300 | 5 000 | 3,2 | – | ▸ 7315 BEP |
| | 160 | 37 | 132 | 104 | 4,15 | 5 300 | 5 300 | 3,2 | ▸ 7315 BECBP | – |
| | 160 | 37 | 132 | 104 | 4,15 | 5 300 | 5 300 | 3,2 | ▸ 7315 BECBY | – |
| | 160 | 37 | 132 | 104 | 4,15 | 5 300 | 5 300 | 3,2 | 7315 BEGAPH | – |
| | 160 | 37 | 132 | 104 | 4,15 | 5 300 | 6 700 | 3,2 | ▸ 7315 BECBM | – |

SKF Explorer bearing
▸ Popular item

416 SKF

Figure 42: Bearing catalogue extract selected bearing reference 7315 BECBP [18]

# References


[1] Machinerie spectacle. URL : http://www.machinerie-spectacle.org/coefficients-de-securite.html.

[2] Matweb. URL : http://www.matweb.com/index.aspx.

[3] Rgm cranes. URL : https://www.rgmcranes.com/crane-parts/range-steel-rope-wire/.

[4] Arcelik A.S. Ac inductuion motor catalogue. URL : http://www.tee.com.tr/UPLOAD/DOCUMENTS/IM-en-17-0.pdf.

[5] Atlanta. Rack and pinion catalogue. URL : https://atlantadrives.com/pdf/atlanta.pdf.

[6] Demag. Guide rollers. URL : https://www.demagcranes.com/fr/produits/technique-dentrainement.

[7] ebitt technologies. Ac inductuion motor catalogue. URL : https://www.ebitteurope.com/pdf/Ebitt-Motor-Katalog-R01.pdf.

[8] DVESTA Electric. Anti-sway controller. URL : https://dvesta.com/en/technical-solutions/special-cranes-functions-in-the-control-systems/anti-sway-controller/.

[9] Keyence. Precision sensor. URL : https://www.keyence.eu/frfr/products/measure/laser-1d/lk-g5000/specs/.

[10] Kurt M. Marshek Robert C. Juvinall. *Juvinall's Fundamentals Of Machine Component Design.* Wiley, 2017.

[11] Telemecanique Sensor. Limit switch. URL : https://tesensors.com/cz/en/product/reference/XCKMR44D1H29.

[12] Telemecanique Sensor. Telemecanique sensors for overhead cranes. URL : https://www.youtube.com/watch?v=PEQbYWrwmD0.

[13] Sensy. Load pins. URL : https://www.sensy.com/fr/axes-dynamometriques.

[14] Sesame. Pgl reducers. URL : https://www.sesamemotor.com/uploads/editor/files/planetary%20gearhead%20catalog%20by%20models/planetary%20gearbox%20PGL%20series.pdf.

[15] SICK. X-position laser. URL : JmZmX2lkPXAyODAyNDkmZmZfbWFzdGVySWQ9cDI4MDI0OSZmZl90aXRsZT1ETDEwMC0yM0FBMjEwMSZmZl9xdWVyeT0mZmZfcG9zPTEwJmZmX29yaWdQb3M9MTAmZmZfcGFnZT0xJmZmX3BhZ2VTaXplPTI0JmZmX29yaWdQYWdlU2l6ZT0yNCZmZl9zaW1pPTkyLjA.

[16] SICK. Y-position laser. URL : JmZmX2lkPXAyMTUyNjMmZmZfbWFzdGVySWQ9cDIxNTI2MyZmZl90aXRsZT1ETDUwLU4yMjI1JmZmX3F1ZXJ5PSZmZl9wb3M9MiZmZl9vcmlnUG9zPTEzNSZmZl9wYWdlPTEmZmZfcGFnZVNpemU9OCZmZl9vcmlnUGFnZVNpemU9OCZmZl9zaW1pPTk0LjA.

[17] SICK. Z-position laser. URL : https://www.sick.com/fr/fr/capteurs-de-distance/capteurs-de-distance-a-moyenne-portee/dx35/dl35-b15552/p/p309059?ff_data=JmZmX2lkPXAzMDkwNTkmZmZfbWFzdGVySWQ9cDMwOTA1OSZmZl90aXRsZT1ETDM1LUIxNTU1MiZmZl9xdWVyeT0mZmZfcG9zPTEmZmZfb3JpZ1Bvcz0yNSZmZl9wYWdlPTEmZmZfcGFnZVNpemU9OCZmZl9vcmlnUGFnZVNpemU9OCZmZl9zaW1pPTk0LjA=.

[18] SKF. Skf selection procedure. URL : https://www.skf.com/group/products/rolling-bearings/principles-of-rolling-bearing-selection/bearing-selection-process/bearing-size.

[19] SmartCrane. Anti sway system. URL : http://www.smartcrane.com/SmartCrane/Documents_files/SmartCraneProducts.pdf.

[20] TGB-Group. Tgb full catalogue drives - ed.5 - l.v. URL : https://www.tgb-group.com/en/slewing-rings-catalogue/thank-you-slewing-rings-catalogue-download/.